Modeling and Dynamics of Coupled Dome-shaped Micromechanical Oscillators

T. Sahai*, and A. Zehnder**

* Department of Theoretical and Applied Mechanics, Cornell University
317 Kimball Hall, Ithaca 14853, NY, USA, ts269@cornell.edu
** Cornell University, NY, USA, atz2@cornell.edu

ABSTRACT

Coupled micromechanical oscillators vibrating in synchrony have the potential for novel applications such as filters, neurocomputers and generators of clock signals in computer processors. In this work we analyze a feasible approach for constructing coupled micromechanical oscillators that synchronize. For this purpose we consider dome shaped micro-oscillators. These oscillators are fabricated by buckling a thin circular film of polysilicon, giving rise to a dome-shaped structure. They are thermally excited using resistive heating. The motion of the device is fed back into the heater using displacement measurement (e.g. capacitive pickup), driving the dome into stable limit cycle oscillations. Here we study the dynamics of one oscillator, and the ability of two micromechanical oscillators with different frequencies to synchronize via mechanical and electro-thermal coupling.

Keywords: mems, modeling, galerkin projection, buckling, coupled oscillators

1 INTRODUCTION

Potential applications for synchronized micromechanical oscillators include signal processing [1], neurocomputing [2] and clock signal distribution for synchronous processors. In this work we develop a theoretical basis for the design of synchronized micro-oscillators. As an example, we analyze thermally excited dome shaped micro-oscillators, fabricated by buckling a thin, circular film of polysilicon [1]. The thin film of polysilicon is first deposited onto a layer of silicon dioxide. The deposition parameters are selected to ensure that the polysilicon is under large compressive (approximately 220 MPa) stress. A circular region of silicon dioxide is etched away leaving a thin polysilicon disk under compression. This disk buckles to form a shallow dome. Typical oscillator diameters range from 10 to 40 μm. For our analysis we use a dome with outer diameter 40μm, inner diameter of 4μm, thickness 200nm and a measured buckled height of 1μm [1] (see Figure 1). We note that there is nothing special about this size and that our analysis can be repeated for domes of different dimensions.

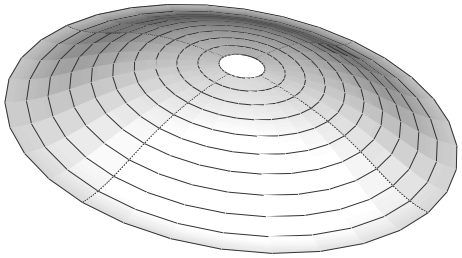

Figure 1: 3D view of the dome obtained from FEM simulations.

In [1] the domes are driven using resistive heating and the motion optically detected [3]. Laser detection of motion may not be feasible for commercial applications, thus, we propose to detect motion using capacitive sensors or strain gauges, fabricated onto the surface of the oscillator. We propose a system in which the output of the displacement sensor is fed back into the resistive heater (Figure 2). This two way coupling of the motion to the thermal dynamics of the oscillator gives rise to limit cycle oscillations as seen in [1]. Before we study the dynamics of coupled oscillators, we need to construct a model for the dynamics of a single oscillator.

2 SINGLE OSCILLATOR MODEL

2.1 Mechanical

To understand the dynamics and mechanical response of a single oscillator, we build an ordinary differential equation (ODE) model for oscillations of the dome about the buckled state. The post buckled shape of the dome is shown in Figure 1. We approximate the shape as

$$w(r) = \frac{1 - \cos(\frac{\pi(r-R)}{R})}{2}, \qquad (1)$$

where r is the radial distance from the center of the dome and R is the outer radius of the dome oscillator, see figure 3. We use the axisymmetric von Kármán equations [4] to describe the nonlinear motion of a plate under compression. The outer boundary of the dome $R = 20\mu$m is considered to be clamped and the inner boundary $r_0 = 2\mu$m is free.

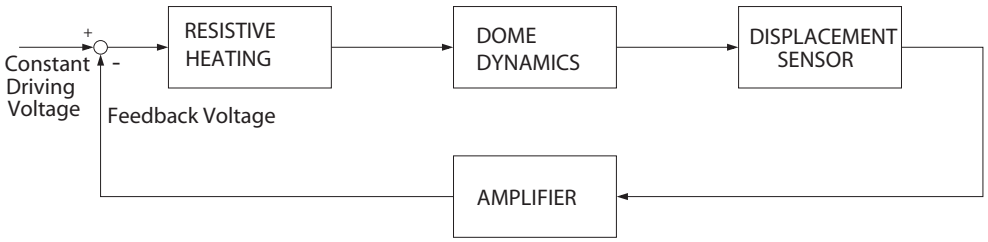

Figure 2: Block diagram of the proposed scheme to construct thermally driven micromechanical oscillators

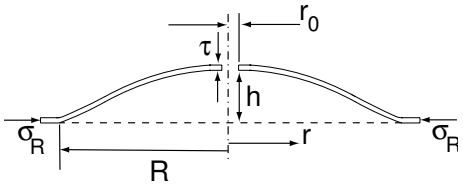

Figure 3: Dimensions of the dome oscillator (view of a radial section)

Table 1: Material Properties of Polysilicon

E	160 GPa
ρ	2330 $\frac{kg}{m^3}$
α	$2.6 \times 10^{-6}/K$
k	20 $\frac{W}{mK}$
C_p	753 $\frac{J}{kgK}$
ν	0.22

We constrain the dynamics of the plate to the mode shape given by Equation 1, by performing a Galerkin projection [4]. The result is a set of nonlinear ODEs that govern the dynamics of the dome oscillator. This ODE is of the form

$$m\ddot{A}(t) + \gamma'\dot{A}(t) + k_1 A(t) + k_3 A(t)^3 = 0, \qquad (2)$$

where m is the effective mass of the structure, γ' is the damping, and k_1 and k_3 are the linear and and cubic stiffnesses calculated using the Galerkin projection procedure. The stiffness k_1 is found to be a linear function of σ_R, the radial stress at the outer edge of the disk, as plotted in Fig. 4. The cubic stiffness, however, is independent of σ_R. The value of σ_R at which $k_1 = 0$ is the buckling load. For the dimensions and properties (from [6], [7] in Table 1) of our problem the critical buckling stress is found to be $\sigma_R \approx 19$ MPa. For $\sigma_R > 19$ MPa, $k_1 < 0$ and the structure assumes a buckled shape. The experimentally observed deflection of the dome is $\approx 1\mu m$ [3], which is found to correspond to $\sigma_R \approx 62$ MPa. Thus, the stress release due to buckling reduces the in-plane radial stress, σ_R, from 220 MPa to 62 MPa.

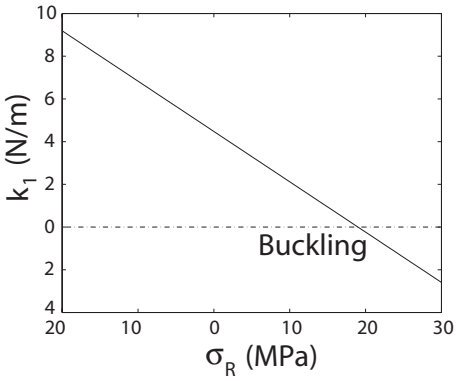

Figure 4: Variation of linear stiffness of plate with applied compressive stress at outer edge. Negative stiffness implies buckling.

The resistive heater causes the dome to deflect upwards. This deflection has contributions from uniform heat expansion and higher compressive stresses at the boundary. We assume linearity and add the two effects. We find that the equilibrium of the structure varies linearly with temperature above ambient. Moving the origin to the buckled state, nondimensionalizing deflection by dividing by the thickness τ of the structure, and nondimensionalizing time gives

$$\ddot{z} + \frac{(\dot{z} - D\dot{T})}{Q} + h(T)(z - DT) + 3\sqrt{\frac{h(T)\beta}{2}}\tau(z - DT)^2 + \beta(z - DT)^3 = 0, \qquad (3)$$

From thermal calculations we get $h(T) = 1 + 0.00023T$. Calculations on height increase give $D = \frac{D'}{\tau} \approx 6 \times 10^{-4}/K$. From the Galerkin projection we get $\beta \approx 0.5$. The quality factor, Q, of the device is found experimentally to be ≈ 2500 [3].

2.2 Thermal

We build a thermal model of the structure by solving transient heat conduction on an annulus,

$$\frac{\partial T(r,t)}{\partial t} = \kappa\left[\frac{\partial^2 T(r,t)}{\partial r^2} + \frac{1}{r}\frac{\partial T(r,t)}{\partial r}\right] + q, \qquad (4)$$

NSTI-Nanotech 2007, www.nsti.org, ISBN 1420061844 Vol. 3, 2007

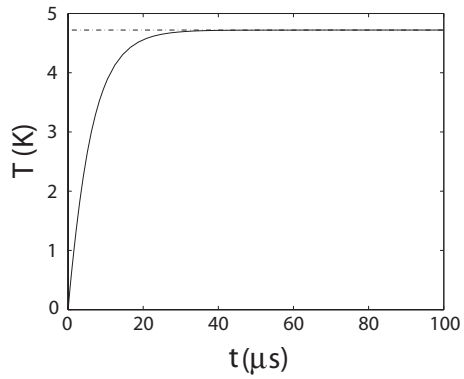

Figure 5: Variation of average temperature of annulus with time.

where q is the heating due to the resistor. Heat loss due to radiation and convection are found to be negligible.

To solve equation 4, we break the solution into two parts: the steady state part and the transient part. The steady state part is the Poisson's equation on an annulus. After solving Poisson's equation, we solve for the transient part, which is the solution of the homogeneous heat equation with appropriate boundary conditions accounting for the steady state part. The solution for equation 4 is a function that depends on radial position and time. We now average this solution over the dome and model the response as a first order ODE,

$$\dot{T} = -B_T T + A_T P, \tag{5}$$

where T is the temperature above ambient, B_T is the rate of cooling due to conduction, A_T is the inverse of the lumped thermal mass and P is the input heat power. From figure 5, we find $A_T = 1.3 \times 10^{-3} \frac{K}{\mu W}$ and $B_T = 1.54 \times 10^{-1}$. Equations 3 and 5 give us a complete thermo-mechanical ODE model for dome dynamics.

3 SINGLE OSCILLATOR DYNAMICS

We model the dynamics of a single oscillator (equations 3 and 5). A close inspection of equation 3 shows that $z = DT$ is an equilibrium. Increasing the input power P increases temperature which in turn deflects the structure. This equilibrium loses stability via a Hopf bifurcation [8] at $P = 2625\mu W$. The limit cycle (self oscillation) born at the Hopf bifurcation gains stability at a saddle-node bifurcation shown in figure 6.

4 COUPLED OSCILLATORS

We select the stable periodic motion at $P = 2585\mu W$ to study the response of two coupled oscillators. We detune one oscillator from the other by changing the frequency of the first by changing the $h(T)$ term. For

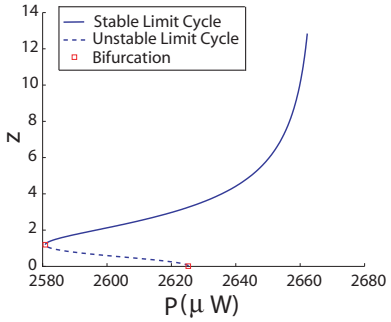

Figure 6: Maximum amplitude of oscillation of dome versus heat input, $z = \frac{w(r_0)}{\tau}$.

the second oscillator the $h(T)$ term becomes $h_2(T) = \kappa + 0.00023T$, where κ is a detuning parameter. We now study the ability of different forms of coupling to frequency lock the two oscillators.

4.1 Mechanical Coupling

In mechanical coupling we assume that the two detuned oscillators are coupled to each other by a spring. Physically this spring can be fabricated beams that connect the oscillators [9]. The governing equations are given by

$$\dot{T}_1 + B_T T_1 - A_T P(1 + c_g z_1) = 0,$$

$$\ddot{z}_1 + \frac{(\dot{z}_1 - D\dot{T}_1)}{Q} + h_1(T_1)(z_1 - DT_1) + 3\sqrt{\frac{h_1(T_1)\beta}{2}}\tau(z_1 - DT_1)^2 + \beta(z_1 - DT_1)^3 = K(z_2 - z_1),$$

$$\dot{T}_2 + B_T T_2 - A_T P(1 + c_g z_2) = 0,$$

$$\ddot{z}_2 + \frac{(\dot{z}_2 - D\dot{T}_2)}{Q} + h_2(T_2)(z_2 - DT_2) + 3\sqrt{\frac{h_2(T_2)\beta}{2}}\tau(z_2 - DT_2)^2 + \beta(z_2 - DT_2)^3 = K(z_1 - z_2). \tag{6}$$

The spring acts a driving force that penalizes the difference between the two oscillators. The spring stiffness normalized by the linear stiffness of the oscillator (K in eqnation 6) determines the ability of the two detuned oscillators to frequency lock. We integrate the system of equations 6 for different values of stiffness K and detuning κ. We then detect frequency locking in the response of the two oscillators. The results are plotted in figure 7.

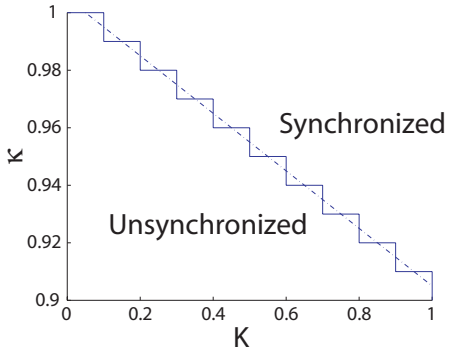

Figure 7: Region of frequency locking of two detuned oscillators with mechanical coupling.

When $\kappa = 1$ the two oscillators are identical and they do not need any spring for frequency locking. Figure 7 displays a linear relationship between the detuning and required stiffness of the spring. The required stiffness increases with detunung. At $\kappa = 0.9$, which corresponds to a frequency difference of 5% between the oscillators, a coupling stiffness of $K \approx 1$ is required.

Fabrication of such arrays of devices is not easy and only nearest neighbor coupling can be achieved. To achieve global coupling between oscillators, we turn our attention to electrical coupling of oscillators.

4.2 Electrical Coupling

In the electrical form of coupling of the oscillators, the motion of one oscillator is converted to an electrical signa that is fed into the resistive heating of the other oscillator. Oscillator 2 thermally drives oscillator 1, without being affected by the dynamics of oscillator 1. The resulting model is given in equation 7. The term ϕz_2 corresponds to the driving seen by oscillator 1 due to the motion of oscillator 2. We now compute the regions where the response of oscillator 1 jumps onto its resonance curve. This region is expected to give frequency locked behavior figure 8. Dynamics in this region is the subject of current study.

$$\dot{T}_1 + B_T T_1 - A_T P(1 + c_g z_1 + \phi z_2) = 0,$$

$$\ddot{z}_1 + \frac{(\dot{z}_1 - D\dot{T}_1)}{Q} + h_1(T_1)(z_1 - DT_1)$$

$$+3\sqrt{\frac{h_1(T_1)\beta}{2}}\tau(z_1 - DT_1)^2 + \beta(z_1 - DT_1)^3 = 0,$$

$$\dot{T}_2 + B_T T_2 - A_T P(1 + c_g z_2) = 0,$$

$$\ddot{z}_2 + \frac{(\dot{z}_2 - D\dot{T}_2)}{Q} + h_2(T_2)(z_2 - DT_2)$$

$$+3\sqrt{\frac{h_2(T_2)\beta}{2}}\tau(z_2 - DT_2)^2 + \beta(z_2 - DT_2)^3 0 = 0, \quad (7)$$

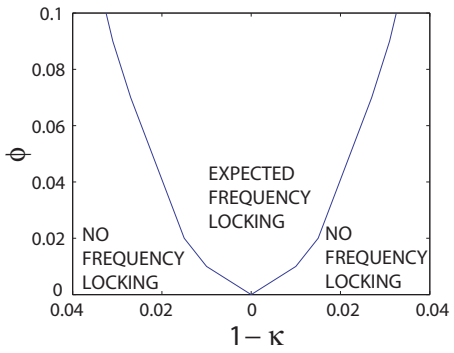

Figure 8: Expected region of frequency locking of two detuned oscillators with electrical coupling.

5 CONCLUSIONS

In this work we take the first steps to model a physical system that can eventually be used for filter applications, neurocomputing [2] or as a means of clock distribution. We select dome oscillators as an example and build a first principles model for the governing mechanical dynamics. Since the oscillator is thermally driven using a resistor, we also build a model for the governing thermal dynamics. A bifurcation analysis of the resulting ordinary differential equations is performed. Stable limit cycle oscillations of the dome oscillator are identified. Two oscillators are then mechanically and electrically coupled and the regions of synchrony are computed by changing the coupling parameter and detuning between the two oscillators.

REFERENCES

[1] R. Reichenbach et. al., J. Micromechanical Systems, 14, 1244-1252, 2005.

[2] F. C. Hoppensteadt and E. M. Izhikevich, IEEE Trans. on Circuits and Systems - I, 48, 133-138, 2001.

[3] M. Zalalutdinov et. al., Applied Physics Letters, 83, 3815-3817, 2003.

[4] Y. C. Fung, Prentice-Hall, 1965.

[5] S. P. Timoshenko and J. M. Gere, "Theory of Elasticity," McGraw-Hill, 1961.

[6] S. Uma et. al., International Journal of Thermophysics, 22, 605-616, 2001.

[7] W. N. Sharpe et. al., Journal of Micromechanical Systems, 10, 317-326, 2001.

[8] J. Guckenheimer and P. Holmes, "Nonlinear Oscillations, Dynamical Systems and Bifurcations of Vector Fields," Springer, 1996.

[9] M. Zalalutdinov et. al., Applied Physics Letters, 78,3142-3144, 2001.